

Research Article

Open Access

Moloshnyi Oleksandr and Szulc Przemyslaw*

The CFD simulation of the flow structure in the sewage pump

<https://doi.org/10.1515/eng-2018-0035>

Received July 6, 2018; accepted August 8, 2018

Abstract: The article presents the results of experimental and numerical tests of a sewage pump. As the object of the research, the single blade impeller was taken into consideration. The primary aim of the project was to investigate the flow structure in the submersible one channel sewage pump by means of the CFD methods. The numerical results were verified on the basis of comparison with experimental results obtained for the real pump. The numerical model was built with good accuracy to the reality and the flow was recognized, which allows creating a new explanation of the working process of the single blade impeller pumps and indicate the possibility of the improvement of the analyzed object. The head curve is characterized by smaller steepness than the results of the experimental tests and the difference, for the best point equals less than 10%. Transient simulation presented fluctuation of the head and power during the impeller rotation cycle. They are 4 m for head and mechanical power – 1 kW. The flow inside the pump was conscientiously analyzed. Pressure and velocity distribution as well as radial hydrodynamic force were presented in the paper.

Keywords: centrifugal pump, single blade pump, hydrodynamic force

1 Introduction

Single-blade pumps are widely used in water supply, industrial sectors and especially for pumping wastewater. The advantage of this pump is the transfer of high pollution water due to the large width of the passageway.

Moloshnyi Oleksandr: Sumy State University, Faculty of Technical Systems and Energy, Applied Hydro- and Aeromechanics Department, Ukraine

***Corresponding Author: Szulc Przemyslaw:** Wroclaw University of Science and Technology, Faculty of Mechanical and Power Engineering, Department of Design Fundamentals and Fluid-Flow Machinery, Poland, E-mail: przemyslaw.szulc@pwr.edu.pl

The complexity of the designing process of a single-blade impeller and casing is to calculate unsteady hydrodynamic processes of fluid flow, which is caused by the not symmetry working elements. In spite of many laboratory tests, there is not sufficient method of designing this kind of hydraulic element. The most effective method of the calculating of a new pump is a recalculation of the existing model pump by means of the laws of the hydrodynamic similarity with some additional corrections in recalculations. In recent years, the research and modernization of this design of the impeller are based on the numerical or real investigations. The widely developed numerical method for the calculation of rotodynamic pumps indicate some problems while the number of blades in the impeller is decreasing. The literature review show some attempts in modeling such geometries. Schiffer et al. [1] have reached better results of the numerical simulation in comparison with experimental using the unsteady method. Souza et al. [2] describe the optimization of single-blade impellers using the design process based on the experiments and computational fluid dynamics methods. Kim et al. [3] proposed a new impeller design method for the single-blade pump and improved the hydraulic performance of the pump. Head, pressure fields, velocity distribution and torque of a single-blade pump based on unsteady simulation and experimental dates were analyzed in articles [4–7]. Pei et al. [8] received high pressure fluctuations near the pressure side of the blade and high gradients of fluctuation values near the trailing edge at the pressure side of the blade. Nishi et al. [9] obtained satisfied comparison of a new analytical approach with the numerical method of designing of the single-blade pump.

Apart from, the hydraulic prediction of the achieved parameters of the pump also the distribution of the radial force, due to the unsymmetrical geometry of the impeller should be taken into consideration. Gulich [10] presented the results of the radial force measurements of the single-blade impellers and gives a recommendation for predicting and minimizing hydraulic excitation forces. Nishi et al. [11] discovered the influence of blade outlet angle to radial trust and determined that bigger outlet angle causing not the only higher head but also the radial trust and

its fluctuation components increases. Benra[12] investigated the dependence of the hydraulic forces from the impeller speed and the flow rate, and in addition, the influence of the hydraulic forces on the pump vibration. Pei et al. [13] (Pei, Dohmen, Yuan, Benra) analyzed hydrodynamic forces on the different part of the impeller and discovered that they are located in second quadrant for the shroud and the blade and third quadrant for the hub.

The literature review shows, that the divergence between the results of the numerical and real experiments is alternating strongly and the authors do not indicate the reasons for this situations. Because of this, authors decided to conduct the appropriate measurements. The main goal of the present paper is to analyze the flow structures of the single-blade impeller pump and to determine the adequacy of pump modeling using a numerical method.

2 Object of the research

To investigate the flow structure in the main passages of a single-blade pump the standard, submersible construction was taken into consideration. The object of the study was presented in Fig. 1. The unit of vertical axis was equipped with a close single-blade impeller. The main parts of the pump were: inlet, impeller and spiral casing. The analyzed pump was characterized by operating and geometrical parameters presented in the Table 1. The unit was described by a value of kinematic specific speed $n_q = n \cdot Q^{0.5} / H^{0.75} = 44 \text{ 1/min}$.

3 Experimental test

To compare the accuracy of the numerical model of the analyzed pump specially prepared test rig was build. The scheme of the measuring stand was presented in Fig. 2. The pump was located horizontally in an open tank, completely filled with water. The medium level and the temperature of water were measured during the tests. The characteristics of the analyzed pump were obtained according to ISO standards [14]. During the test the following parameters were measured:

- Rate of flow – Q – electromagnetic flow meter in accuracy class 0.1.
- Delivery pressure – p_d – electronic pressure gauge in accuracy class 0.6.
- Power consumption – P – power monitoring unit in accuracy class 0.5.

Tests were carried out to obtain the hydraulic properties of the pump.

4 The numerical model

In order to investigate the operating process of analyzed pump the application of the computational flow dynamic was necessary. The main purpose of this stage was to obtain the pressure and velocity fields of the liquid flow. The numerical simulations of the flow in the hydraulic part of the pump were realized using commercial ANSYS CFX software. The numerical model contained four fluid domains: suction pipe, impeller, volute and pressure pipe (Fig. 3). The length of the suction pipe equals for times the diameter of the impeller eye and the discharge pipe - four times the outlet diameter of the volute casing. During the experimental tests, similar inlet pipe was added to the analyzing unit at the inlet side. During the CFD calculation, the gap between the tips of the impeller shroud and the pump casing was neglected. The unstructured mesh was created by means of the ICEM CFD. Tetra elements were made in the center of the flow body and the prisms layers were applied near the walls (first layers equaled 0.025 mm). The density of the mesh increased near the blade. The total number of nodes was assumed in accordance to the test of the mesh independence and it was equaled 6 mln. As the interface between stationary and rotating domains stage average velocity was applied. The boundary conditions were defined as the mass flow rate in the inlet and opening pressure and direction at the outlet of the model. The numerical simulations were carried out as steady as so as unsteady. The pumping medium was water at the temperature 25 °C. The standard models of turbulence $k-\epsilon$ were used for the calculations. The numerical model does not reflect the roughness of the flow parts.

5 Analyses of the results and discussion

To assess the accuracy of the prepared numerical model the comparison between the steady state numerical simulation and the experimental results was made. It is only one correct method to evaluate the accuracy of the model and the reality. The study was based on the measurements of the pump performance made at the test rig (Fig. 2) and then, preparing and realizing the numerical simulation.

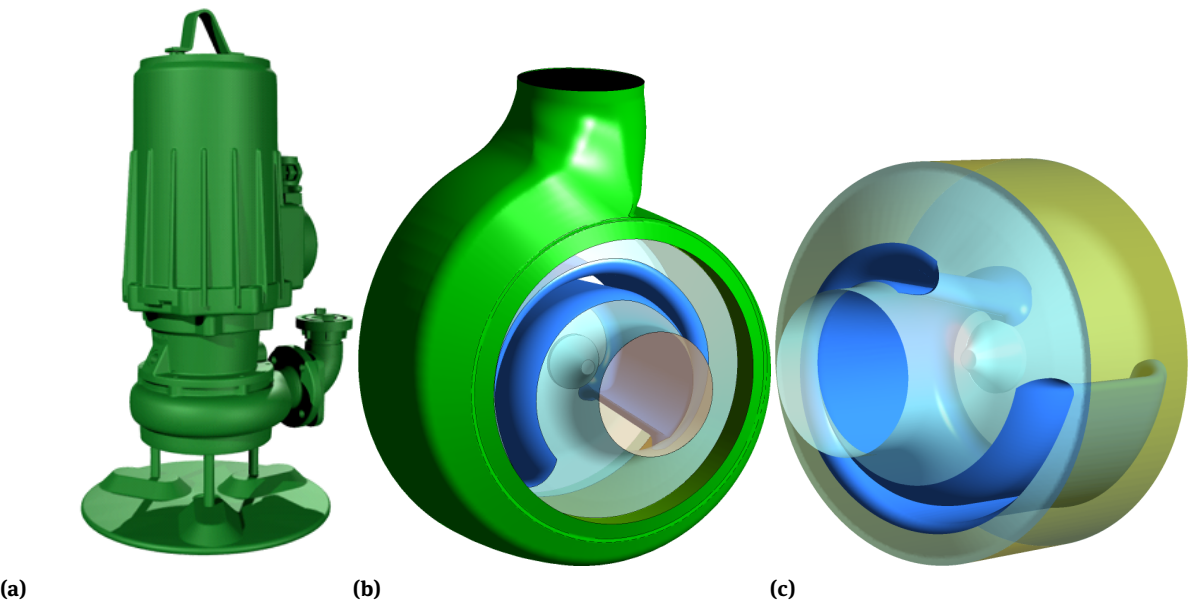


Figure 1: 3D model a) single-blade pump b) impeller and volute; c) impeller

Table 1: Operating and geometrical parameters of the analyzed single-blade pump

No.	Name	Symbol	Value
Operating parameters			
1	Flow	$Q \text{ (m}^3/\text{h)}$	85
2	Total head	$H \text{ (m)}$	8.6
3	Rotational speed	$n \text{ (rpm)}$	1450
4	Power consumption	$P \text{ (kW)}$	4
Geometrical characteristic of the impeller			
1	External diameter	$d_2 \text{ (mm)}$	220
2	Inlet diameter	$d_1 \text{ (mm)}$	100
3	Angular blade grip	$\alpha \text{ (}^\circ\text{)}$	270

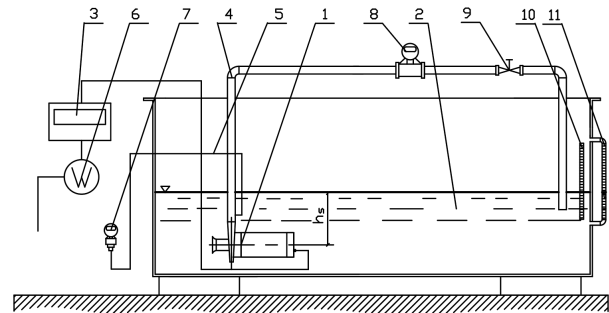


Figure 2: The scheme of the test rig: 1 – model pump, 2 – open tank, 3 – control box, 4 – discharge pipe, 5 – elastic pipe, 6 – power meter, 7 – manometer, 8 – flowmeter, 9 – regulation valve, 10 – thermometer, 11 – level indicator with bypass

In Fig. 4 the comparison of the results of the numerical calculations and experimental tests in relative coordinates

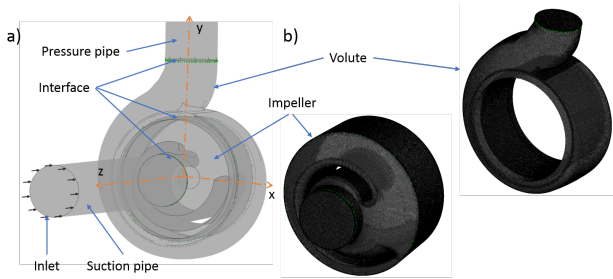


Figure 3: Computational model: a) geometry ; b) mesh

was shown. The flow curve for both research methods is stable, the head is decreasing while raising the flow. It is possible to notice the difference in the shape between the curves of the flow characteristic. The experimental curve has higher steepness then obtained from CFD modeling. As a reason for this situation could be the small differ-

ences in geometries, because the 3D model might not reflect the real geometrical parameters of the existing impeller. Moreover, the alterations in roughness could have an impact on the archived outcomes. In the best efficiency point (BEP), the difference between the numerical modeling and the reality equals approximately 10% and is raising up to 30% while raising the flow value. The power consumption curve measured in real test rig has a similar trajectory to one received from CFD modeling. Numerical investigation outcomes are located lower than the real one. Slight difference between the real and numerical result, near the BEP, equals less than 10% and it is raising with the flow. The reasons are the same as described above. Because of this the BEP, obtained from CFD methods is shifted to higher flows, and the maximum efficiency is higher than one from the real test, but near the real BEP the difference is less than 10%.

The results of the transient simulation with appropriate graphic blade position image was presented in Fig. 5. The graph shows the pulsation of head (H) and power (P_m) on the shaft at a flow rate Q_{BEP} . The peak-to-peak height value is about 4 m, the average value is 10.3 m, which is bigger than for steady state simulation to 3%. The highest values were obtained to the position in which the trailing edge of the blade is located opposite to the tongue of the casing. The smallest value corresponds to the position when the trailing edge is passing the tongue of the spiral. Similar in shape of the curve, shifted a little to smaller rotation angles, could be observed for the power dependence of the blade position. The peak-to-peak height value is about 1 kW. The sharp increase of shaft power of the pump is observed when the trailing edge in passing the tongue. This does not correspond to the relevant peak of the head.

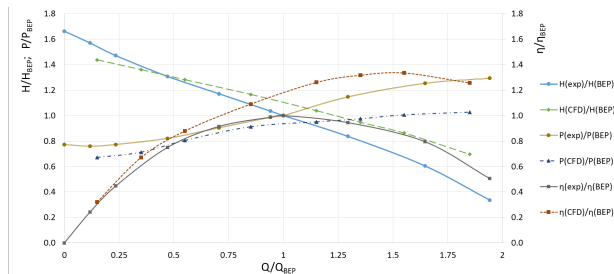


Figure 4: The comparison of the experimental and the numerical results

For a more detailed analysis of the pumps workflow, the pressure distribution and vectors in the chosen cross section of the pump for the selected positions of the impeller (Fig. 5) are presented in Fig. 6 and 7 respectively.

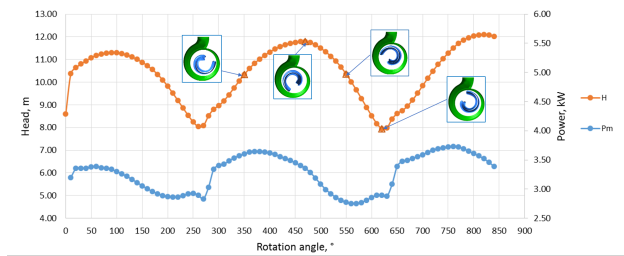


Figure 5: The head and power fluctuation in a function of the blade position

Cross section of the pump is approximate in the center of the impeller. The global pressure distribution strongly depends on the position of the impeller. For the relative coordinate system, the view of pressure zones around the pressure and suction side of the blade is similar for all positions, of course, it rotates along the main axis of the impeller. Usually in the middle of the pressure side of the blade is visible the zone of the higher pressure. Near the leading and trailing edges are the zones of the lowered pressure, which is the consequence of the natural flow of an airfoil. The second zone is also caused by high speed near the trailing edges. It is important to notice, that there is always clearly visible a zone of the least pressure between leading edge, the suction side of the blade and the fairing. Its position is altering in a function of the position of the impeller. The occurrence of this vortex region determines the pressure and velocity distribution behind the suction side of the blade. The indication point of this vortex is located in the area of the lowest pressure in the pump – dynamic depression zone. Then the vortex is shifted to the inlet of the impeller. Thanks to the representation of the velocity vectors, a vortex zone before the leading edge is clearly visible. It was presented in Fig. 7.

Schiffer and Kim [1, 3] also discovered strongly pronounced vortex-regions around the leading edge. In their opinion, it causes a stagnant zone between the leading edge, the suction side of the blade and the fairing. The conscientious analysis of the presented figures allows drawing the following conclusion. The appearance of mentioned vortex structure allows dividing the flow part of the impeller into two elements. One could be called active due to the fluid transportation, and the second one, where the transport of liquid is strongly reduced (region of vortex) – passive part. Both regions were presented in Fig. 8. The vortex is responsible for two advantages. First of all, the external boundary of this phenomenon could be treat as a second blade (red, dashed line in Fig. 8), which allows creating the diffuser channel in the impeller. This thesis is confirmed by the pressure distribution in fig. 6. The second

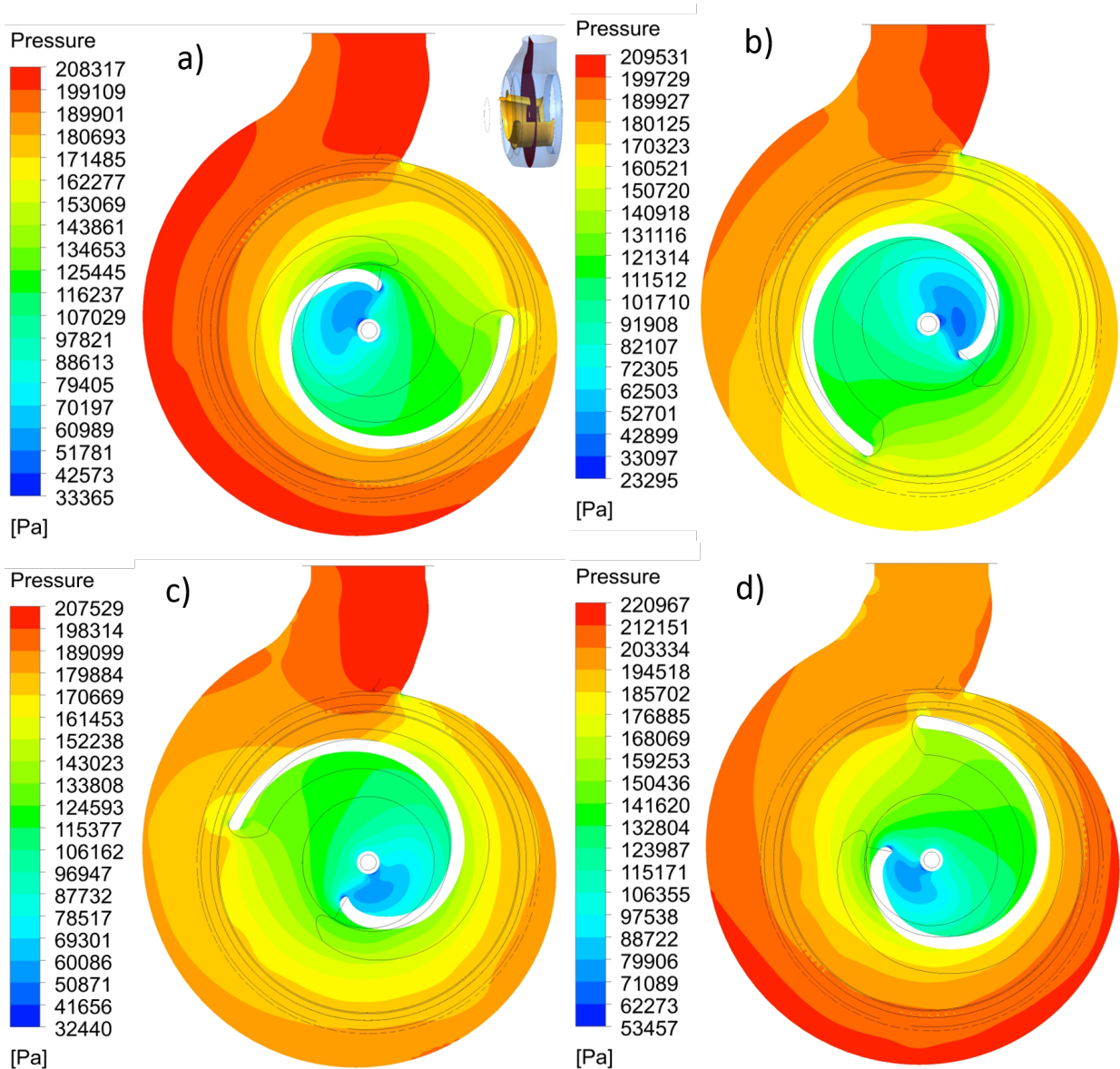


Figure 6: Pressure distribution in the middle cross-section of the pump, the position of the impeller: a) 350°; b) 470°; c) 550°; d) 620°

role is to limit the flow value in the pump. Normally it could be done by means of the construction of spiral casing. Due to the necessity of application of large cross-sections in a spiral, the BEP will be obtained for a very high discharge, and an indication of such vortex allows to shift the BEP to lower flows, without the risk of clogging the impeller or the spiral casing.

At different positions of the impeller, between the pressure side of the blade and the walls of the spiral casing, the diffuser character of the flow could be noticed. The intensify of the energy conversion process depends strongly at the blade position, and it is deteriorated when the blade is passing the tongue of spiral – Fig. 6.

The spiral casing is operating properly, there are visible some deteriorations near the tongue, but it is the normal operation of this kind of element.

Another interesting issue, concerning the operation of the single blade pump, is the value and position of the radial force ($F = (f_x^2 + f_y^2)^{1/2}$). In Fig. 9 was presented calculated radial hydrodynamic force in a function of the position of the impeller. Graphically marked subfigures are corresponding to the positions of the blade that have been considered before. As it can be concluded there is an imbalance of hydrodynamic forces. The amplitude of the quantities is about 1450 N for the vertical (Y) axis and 1400 N for the horizontal (X) one. The center of hydrody-

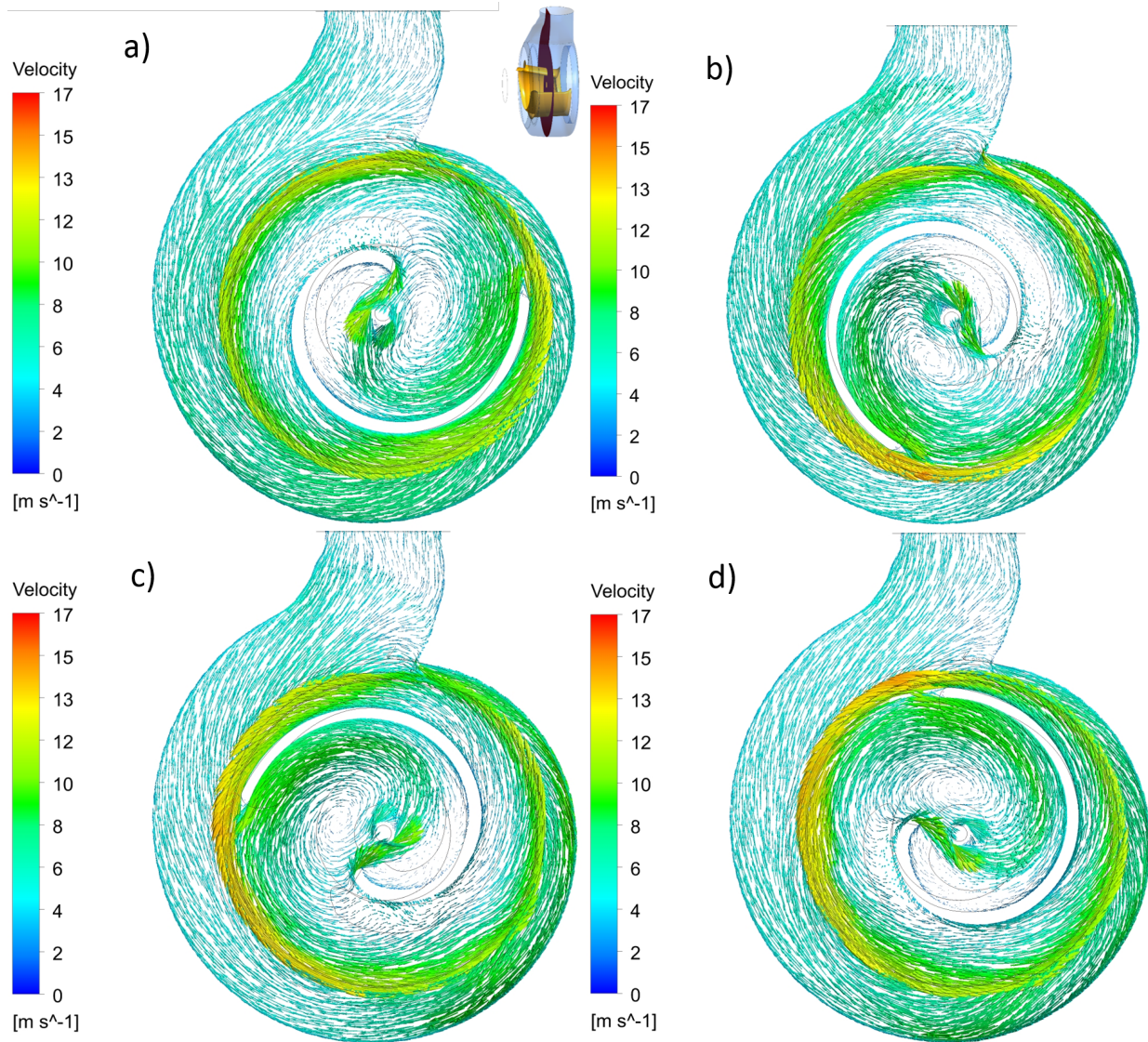


Figure 7: Velocity distribution in the middle cross-section of the pump, the position of the impeller: a) 350°; b) 470°; c) 550°; d) 620°

dynamic forces is shifted from the axis and causing additional vibrations. As it could be seen, the hydraulic forces are growing with the number of the rotation of the impeller, what suggests the necessity of further calculations.

6 Conclusions

Results of the experimental, transient and steady state numerical simulation of the single-blade impeller pump were presented in this paper. In accordance with the conducted analyses and presented results of the investigation other conclusions could be drawn:

- The obtained accuracy for the computational model could be considered satisfactory. This model may be used for a further application and is sufficiently accurate to explain the fluid flow structure.
- The head curve is characterized by smaller steepness than the results of the real investigations. It could be explained by the differences in real and numerical geometry.
- The shape of the compared curves is similar. The CFD performing curves are located above the experimental results. In the entire analyzed range the difference between the results of the numerical calculations and the experimental tests, for the BEP, equals less than 10%.

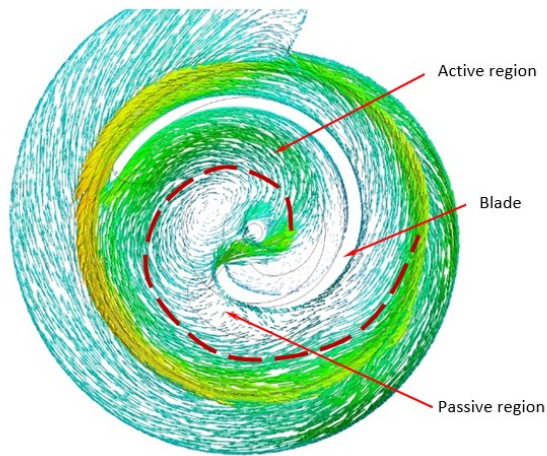


Figure 8: The velocity distribution and the division of fluid sections in the impeller

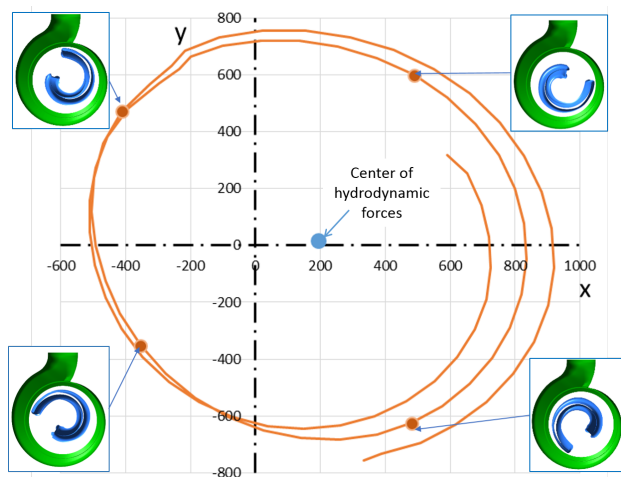


Figure 9: Radial hydrodynamic force, [N]

- Moreover, the simplification of the numerical model could lead to the increase of the value of the head, efficiency, and decline of power consumption. Those simplifications do not have an impact on the flow structure in the impeller and the vane diffuser.
- Transient simulation gives a good representation of the head and power fluctuations during the impeller rotation cycle. The analysis of received outcomes allows describing the correlation between the position of the blade relative to the volute and the largest, smallest and average value of the head. The amplitude of the changes of the head is about 4 m and power – 1kW.
- Due to a detailed analysis of pressure distributions and vectors in the cross-sections of the pump, a vortex zone near the leading edge as well as the zone of

low pressure near were found. This vortex decreases the flow and creates the artificial blade channel.

- For all the positions of the impeller, the hydrodynamic imbalance of the single-blade impeller pump was identified.
- Reducing the amplitude of the pressure fluctuation by changing the blade geometry based on the results of the structure of the fluid flow is the next task of execution.

Acknowledgement: This research was supported by the Visegrad Fund. The authors are grateful for the financial support.

Calculations have been carried out using resources provided by Wroclaw Centre for Networking and Supercomputing (<http://wcss.pl>), grant No. 444/2017.

References

- [1] Schiffer J., Bodner C., Jaberg H., S. Korupp, Runte L., Performance analysis of a single-blade impeller pump based on unsteady 3D numerical simulation, International Rotating Equipment Conference, Düsseldorf, 2016.
- [2] Souza B., Niven A., and Daly J.: Single-blade impeller development using the design of experiments method in combination with numerical simulation. Proc. IMechE Vol. 222 Part E: J. Process Mechanical Engineering, 2008, 135-142.
- [3] Kim J.-H., B.-M. Cho, Kim Y.-S., Choi Y.-S., Kim K.-Y., Kim J.-H. and Cho Y.: Optimization of a single-channel pump impeller for wastewater treatment, International Journal of Fluid Machinery and Systems, 2016, 9(4), 370-381.
- [4] Ala-Juusela J., Study of boundary conditions in single-blades pup simulation, not published, 2007, 25.
- [5] Souza B., Daly J., Niven A. and Frawley P.: Numerical simulation of transient flow through single blade centrifugal pump impellers with tipgap leakage. Proceedings of the 4th WSEAS International Conference on Fluid Mechanics and Aerodynamics, (Elounda, Greece), 2006, August 21-23, Elounda, 349-354.
- [6] Ji P., ShouQi Y. and JianPing Y., Numerical analysis of periodic flow unsteadiness in a single-blade centrifugal pump, Science China, Technological Sciences, 2013, 56(1), 212–221.
- [7] Pei J., Yuan S. and Yuan J., Fluid-structure coupling effects on periodically transient flow of a single-blade sewage centrifugal pump, Journal of Mechanical Science and Technology 2013, 27 (7).
- [8] Pei J., Yuan S., Benra F.-K., Dohmen H. J., Numerical prediction of unsteady pressure field within the whole flow passage of a radial single-blade pump, Journal of Fluids Engineering, 2012, 134.
- [9] Nishi, Y., Fujiwara, R., Fukutomi J., Design method for single-blade centrifugal pump impeller, Journal of fluid science and technology, 2009, 4(3), 786-799.
- [10] Gülich, J.F., Centrifugal Pumps, 3rd Edition, 2014, Springer.
- [11] Nishi Y., Fukutomi J., Fujiwara R., Effect of blade outlet angle on radial thrust of single-blade centrifugal pump, 26th IAHR Sym-

- posium on Hydraulic Machinery and Systems, IOP Conference Series: Earth and Environmental Science, 2012, 15.
- [12] Benra F.-K., Numerical and experimental investigation on the flow induced oscillations of a single-blade pump impeller, *Journal of Fluids Engineering* Copyright, 2006, 128, 783-793.
- [13] Pei J., Dohmen H.J., Yuan S.Q., Benra F.-K., Investigation of unsteady flow-induced impeller oscillations of a single-blade pump under off-design conditions, *Journal of Fluids and Structures*, 2012, 35, 89–104.
- [14] EN ISO 9906: 2012 (E), Rotodynamic pumps — Hydraulic performance acceptance tests — Grades 1, 2 and 3, 2012.